frontiers | Frontiers in Earth Science

TYPE Original Research
PUBLISHED 28 April 2025
DOI 10.3389/feart.2025.1586275

OPEN ACCESS

EDITED BY
Yu Zhuang,
WSL Institute for Snow and Avalanche Research SLF, Switzerland

REVIEWED BY
Zhao Duan,
Xi'an University of Science and Technology, China
Yanqiu Leng,
Chang'an University, China

*CORRESPONDENCE
Jinkai Yan,
yanjinkaisw@163.com
Zejun Xia,
xia1985@163.com

RECEIVED 02 March 2025
ACCEPTED 10 April 2025
PUBLISHED 28 April 2025

CITATION
Wei G, Yan J, Xia Z, Li B and Qi H (2025) Research on the instability mechanism of loess landslides based on preferential infiltration of rainfall.
Front. Earth Sci. 13:1586275.
doi: 10.3389/feart.2025.1586275

Research on the instability mechanism of loess landslides based on preferential infiltration of rainfall

Gang Wei[1,2], Jinkai Yan[3]*, Zejun Xia[1,2]*, Bin Li[4,5] and Huawen Qi[1,2]

[1]Qinghai Environmental Geological Prospecting Bureau, Key Laboratory of Environmental Geology of Qinghai Province, Xining, China, [2]Qinghai 906 Engineering Survey and Design Institute, Xining, China, [3]Chinese Academy of Geological Sciences, Beijing, China, [4]The First Non-ferrous Geological Exploration Institute of Qinghai Province, Xining, China, [5]College of Geology and Environment, Xi'an University of Science and Technology, Xi'an, China

Loess landslides represent a prevalent and severe type of geological disaster in the Loess Plateau and its surrounding regions. Their frequency and intensity are notably exacerbated under rainfall conditions. This study focuses on investigating the destabilization mechanism of loess landslides induced by rainfall preferential infiltration on the northern slope of the Xining Haihu Bridge. A combination of on-site monitoring, soil property testing, and numerical simulations was employed. The findings reveal that during rainfall events, water rapidly infiltrates into the deep soil layer through pre-existing preferential pathways, such as cracks. This alters the internal water distribution within the soil, leading to localized slope saturation. The subsequent increase in pore water pressure and substantial reduction in soil shear strength emerge as critical factors in triggering loess landslides. Additionally, numerical simulation models were utilized to analyze slope stability under varying rainfall scenarios. The analysis identifies key factors influencing the stability of loess landslides, namely rainfall intensity, duration, and the position and depth of cracks. Furthermore, this study innovatively integrates quantitative analysis of rainfall-induced preferential infiltration with dynamic simulations of landslide stability. This approach offers a more robust theoretical foundation for predicting, assessing, and mitigating loess landslides. By quantifying the relationship between landslide stability and rainfall infiltration patterns, the study provides vital technical support for early warning systems, disaster prevention strategies, and the optimization of engineering measures aimed at addressing loess landslide hazards.

KEYWORDS

loess landslides, preferential infiltration, rainfall, slope stability, numerical simulation

1 Introduction

Loess landslides are common and highly hazardous geological disasters in the Loess Plateau (Liu et al., 2024), especially in the northwestern regions of China. These landslides frequently occur, severely affecting regional infrastructure, traffic safety, and human life and property safety. The causes of loess landslides are complex,

FIGURE 1
Geographic location of study area.

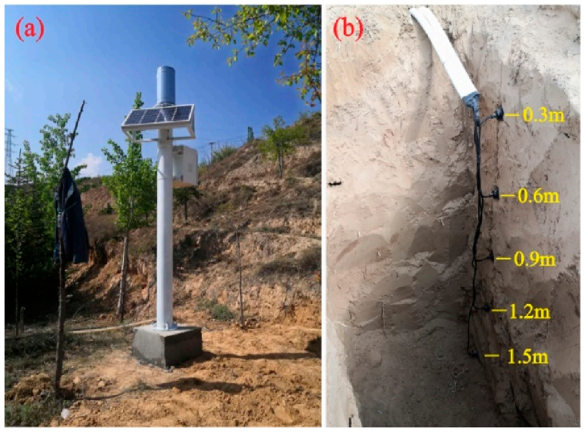

FIGURE 2
(a) integrated rainfall and soil moisture monitoring instrument; **(b)** layout of soil moisture monitoring sensors.

TABLE 1 Calculation model summary.

Numbers	Types	Locations	Depths
1	No-crack model		
2	Crack model	Back	10 m
3	Crack model	Back	15 m
4	Crack model	Back	20 m
5	Crack model	Middle	10 m
6	Crack model	Middle	15 m
7	Crack model	Middle	20 m
8	Crack model	Front	10 m
9	Crack model	Front	15 m
10	Crack model	Front	20 m
11	Crack model	Front, middle, and back	10 m
12	Crack model	Front, middle, and back	15 m
13	Crack model	Front, middle, and back	20 m

involving internal and external factors. Internal factors are primarily related to the unique geological characteristics of loess, such as high moisture sensitivity, low strength, and high porosity (Duan et al., 2024). These soil properties cause the strength of loess to rapidly decrease when it encounters water, making it prone to landslides (Hu, 2013; Hou et al., 2024). In addition, loess areas often exhibit significant crack systems, such as vertical joints, unloading joints, and structural joints, which provide pathways for water infiltration, further exacerbating loess instability (Zheng et al., 2007; Li et al., 2018a). External factors mainly include rainfall, groundwater level changes, and human activities. Among them, rainfall is one of the primary triggers for loess landslides. Studies show that heavy rain or continuous rainfall increases soil saturation, raising the likelihood of landslides (Zhang et al., 2019; Li et al., 2020; He et al., 2023; Wang et al., 2024).

In recent years, preferential infiltration has become an important research direction in loess landslide studies. Preferential infiltration refers to the rapid downward infiltration of water through significant pathways in the soil, such as cracks, joints, and sinkholes, which accelerates deep water infiltration and causes certain areas of the soil to rapidly saturate, leading to a reduction in strength (Zhang et al., 2019). Under low-intensity rainfall conditions, water typically infiltrates the soil evenly and slowly. However, under high-intensity rainfall or heavy rain conditions, surface runoff may form, and water rapidly infiltrates through larger pores, cracks, or sinkholes, a phenomenon known as preferential infiltration (Butler and Gillham, 1996; Zhang et al., 2019), where rainwater rapidly infiltrates through cracks in the soil, thus rapidly altering the localised moisture distribution of the slope and affecting the stability of the slope (Zhang et al., 2019; Feng, 2020; Yan et al., 2020).

Rainfall-induced preferential infiltration leads to rapid soil saturation in certain soil areas, especially near sliding surfaces, increasing pore water pressure as well as a significant reduction in the shear strength of the soil, which threatens the stability of slopes (Zhang S et al., 2017; Feng, 2020; He et al., 2024). As preferential infiltration rapidly changes the soil water distribution, it affects the soil physico-mechanical properties. Especially in areas prone to loess landslides, rainfall-induced preferential infiltration is prone to trigger loess landslides (Mirus and Benda, 2010; Li et al., 2018b).

There is limited research on how preferential infiltration induced by rainfall contributes to landslide instability in loess areas, especially regarding the quantitative impact of the location and depth of preferential infiltration channels on slope stability (Kang et al., 2017). This study uses field monitoring, experimental testing, and numerical simulations to investigate the patterns of preferential infiltration and its impact on slope stability in loess landslides. The aim is to uncover the mechanism behind landslide instability caused by preferential infiltration and provide scientific support for the prevention and risk assessment of loess landslides.

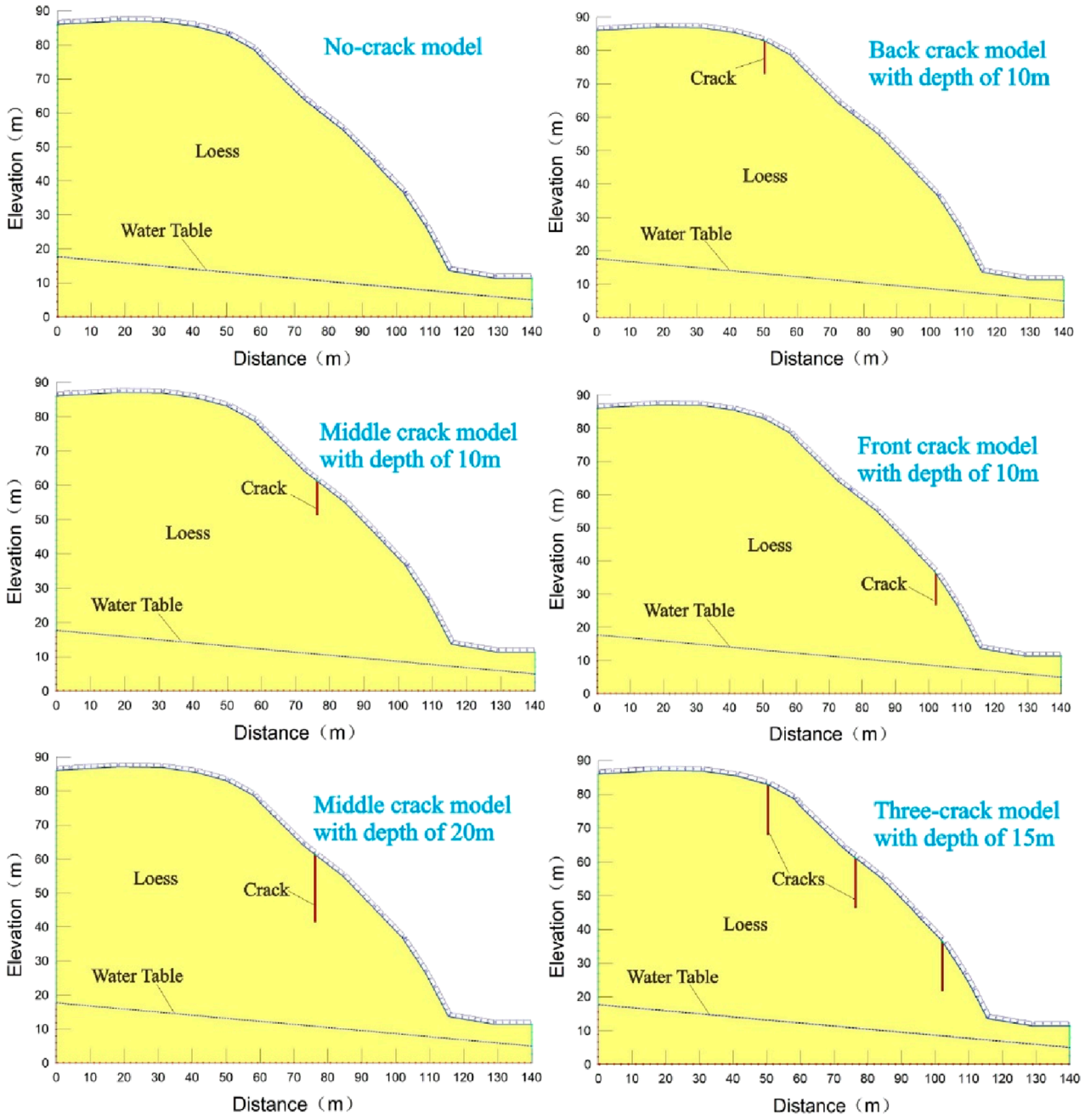

FIGURE 3
Calculation model diagram.

2 Study area geology

2.1 Geographic location

This study focuses on the loess slope located north of Haihu Bridge in the northern district of Xining, Qinghai Province. The area is north of Xining City, adjacent to the Yushu Tax Bureau New Oasis Community, specifically on the slope north of the former Xining Wind Turbine Factory (Figure 1). The study area is conveniently located next to the city's main transportation routes and is a typical sample for studying loess landslides, providing representativeness and research value.

2.2 Topography and landforms

The Haihu Bridge North landslide is in the transitional zone between the hilly and river valley regions. The overall terrain of the

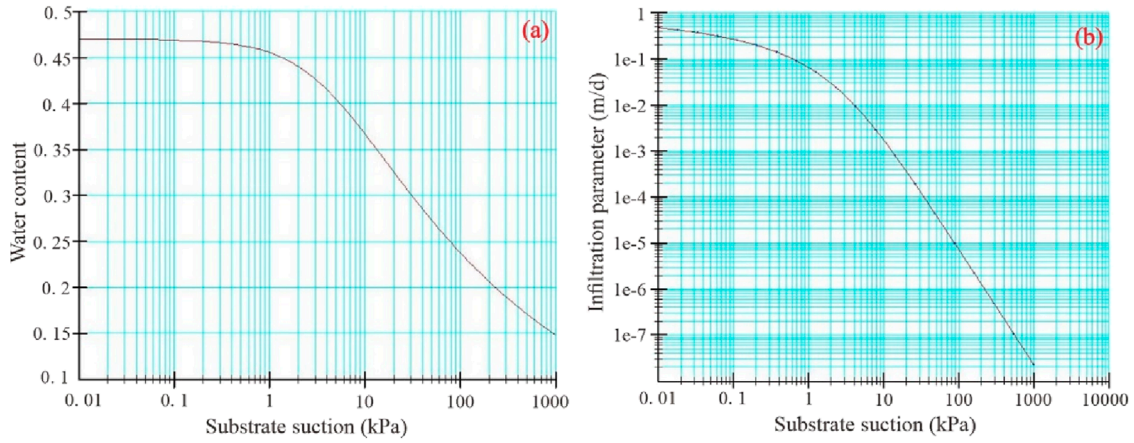

FIGURE 4
Loess infiltration calculation parameters **(a)** Soil-water characteristic curve. **(b)** Unsaturated permeability.

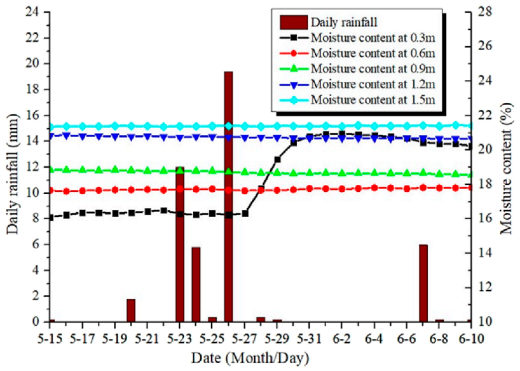

FIGURE 5
Relationship between daily rainfall and soil moisture from May 15 to 10 June 2023.

area shows a north-high, south-low slope. Based on the genesis and morphological features of the landforms, the region can be divided into two main types: low mountain hills and accumulated river valley plains. The northern part of the study area consists mainly of erosion-exhumation low mountain hills, which have been subjected to tectonic pressure and have been uplifted for a long time. The elevation of this area ranges from 2,200 to 2,350 m, with a relative height difference of 70–120 m. The geological composition includes Quaternary upper Pleistocene aeolian loess, gravel, and mudstone. The mountain slopes are steep, and the valleys are well-developed. Due to human interventions, small drainage channels have formed at the front of the research slope, increasing the risk of collapse and making these areas potential high-risk zones for geological disasters (Yang et al., 2016).

The accumulated river valley plain was formed due to long-term crustal subsidence, which has undergone significant sinking and been compensated by deposits of various origins. This plain is primarily distributed south of the hills, including the New Oasis Community in Yushu Tax Bureau. The study area is about 400 m from the Huangshui River, located in the transition zone between the low valley and the hilly regions. The terrain is relatively steep, with intersecting valleys, making it prone to landslides and other geological hazards (Wu et al., 2015).

2.3 Climatic conditions

The study area is in a plateau continental climate zone characterized by intense sunlight and significant diurnal temperature variations. The region experiences relatively low and uneven precipitation. According to the Xining Meteorological Observatory data, the average annual rainfall in the study area is approximately 345 mm, with precipitation mainly concentrated between June and September, accounting for more than 80% of the annual rainfall. Heavy rainfall events are frequent during this period, especially short-duration, intense rainstorms. Statistical analysis of the meteorological data over the past 30 years shows that the area recorded 12 intense rainfall events with hourly rainfall exceeding 20 mm and six heavy rain events with daily rainfall reaching or exceeding 50 mm. These intense rainfall events directly affect the stability of the slopes (Zhang Y et al., 2017).

2.4 Stratigraphic structure

The stratigraphy of the Haihu Bridge North Slope consists of the following layers, from top to bottom: Quaternary upper Pleistocene loess and Paleogene mudstone. The specific stratigraphic characteristics are as follows:

Quaternary Upper Pleistocene Aeolian Loess (Q_3^{eol}): This layer is mainly distributed in the hilly region's northern part of the study area, showing a yellowish color with large pores and well-developed vertical joints. It contains calcareous nodules and exhibits collapsibility. The maximum thickness of this layer reaches 84.4 m.

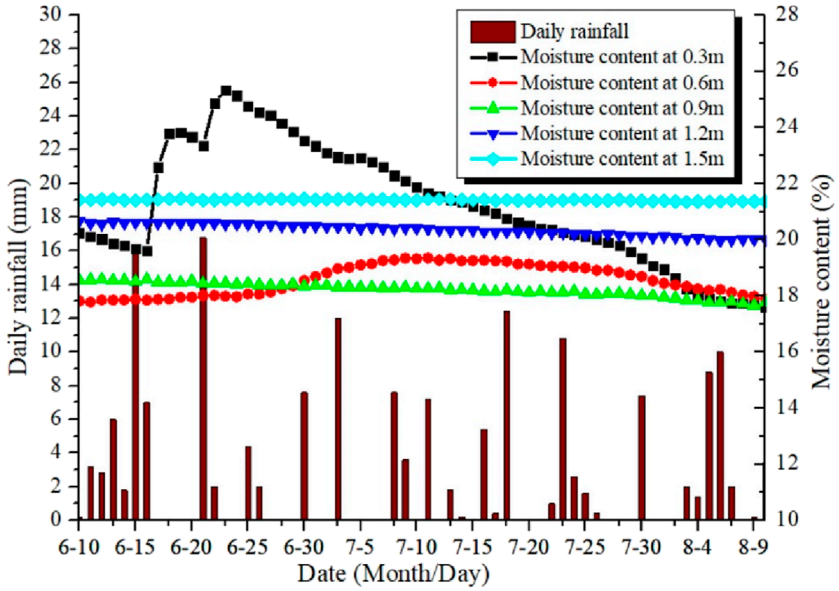

FIGURE 6
Relationship between daily rainfall and soil moisture from June 10 to August 10.

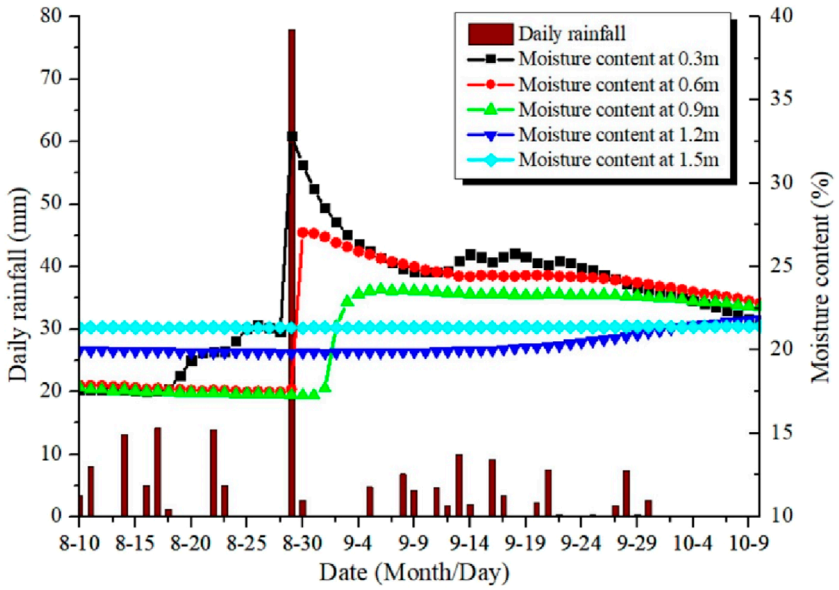

FIGURE 7
Relationship between daily rainfall and soil moisture from August 10 to October 10.

Paleogene Mudstone (E): This layer is sporadically distributed in the third-level terrace of the river valley plain area at the foot of the slope in the study area. The color is brick-red and slightly moist, and the structure is relatively dense. The thickness of the strongly weathered layer typically ranges from 5 to 8 m and exhibits a mudstone structure and blocky texture. Joints and fissures are well-developed in the weathered layer, with filled silt and fine sand visible in the cracks.

3 Research methods

3.1 Field monitoring of rainfall infiltration

Field monitoring was conducted to study the infiltration patterns under natural conditions. The monitoring equipment used was an integrated rainfall and soil moisture monitoring instrument consisting of five components: sensors, an intelligent data collector, a controller, a solar panel, and a battery, as shown in Figure 2a.

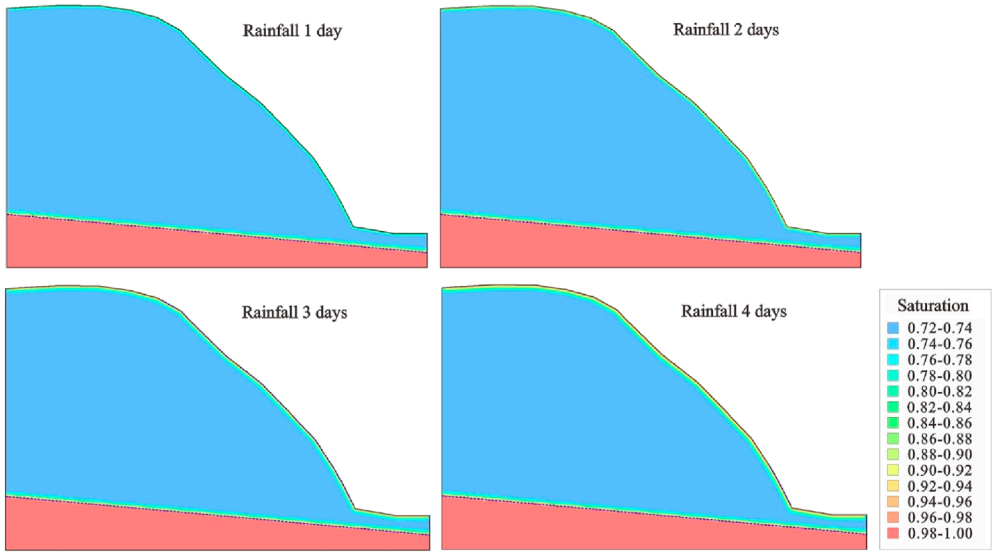

FIGURE 8
Saturation maps of the loess slope under regular rainfall (30 mm/d).

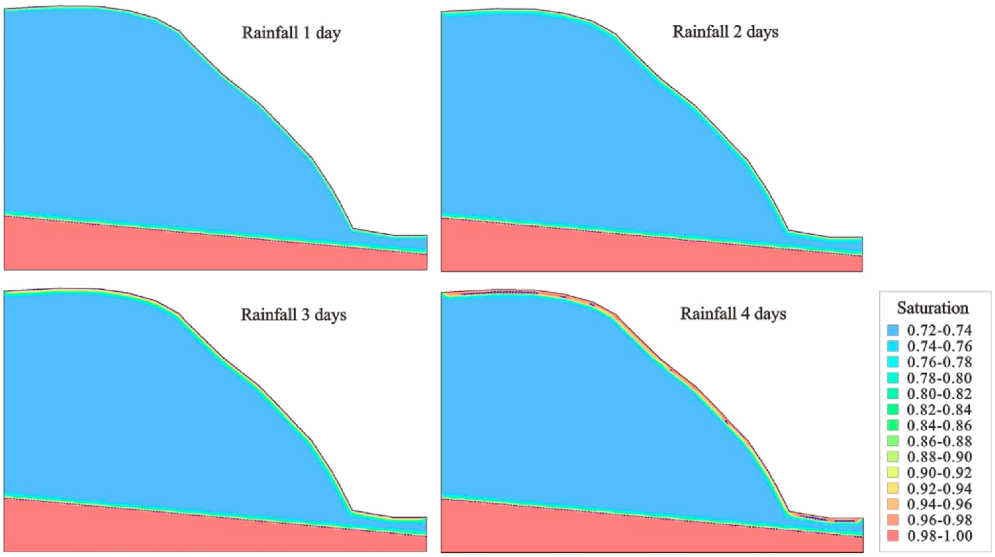

FIGURE 9
Saturation maps of the loess slope under extreme rainfall (70 mm/d).

The soil moisture monitoring instrument has five sensors installed at different depths (0.3, 0.6, 0.9, 1.2, 1.5 m), with the layout shown in Figure 2b. This monitoring equipment obtained real-time measurements of rainfall and soil moisture changes at different depths, providing field data for studying the infiltration patterns under rainfall conditions. This monitoring method enables direct observation of moisture changes at different soil depths and further analysis of water infiltration characteristics under rainfall conditions (Chen et al., 2019).

3.2 Numerical simulation modeling scheme

Since obtaining the complete rainfall preferential infiltration patterns through field monitoring is challenging, this study used the Seep/W module in Geostudio software to simulate the rainfall infiltration patterns of loess slopes considering preferential infiltration channels. The flow results were then overlaid on the slope stability calculation model, and the Slope/W module was used

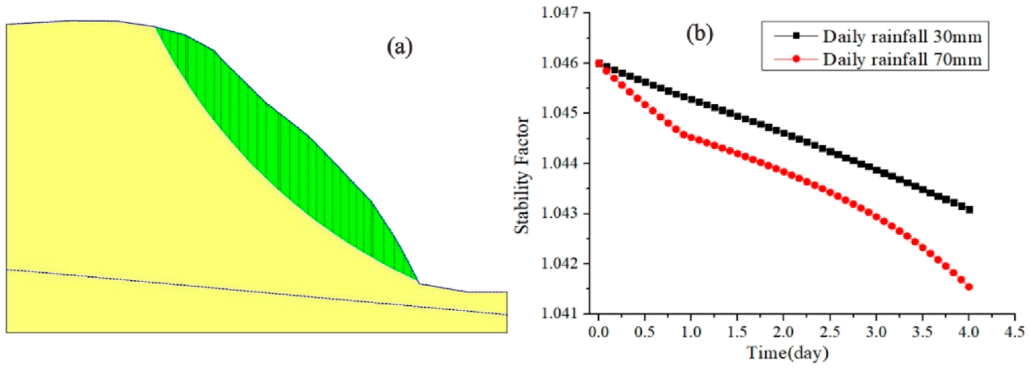

FIGURE 10
Calculation results of the stability of the no-crack model under rainfall conditions. **(a)** The most dangerous sliding surface of the slope; **(b)** Stability factor variation curve.

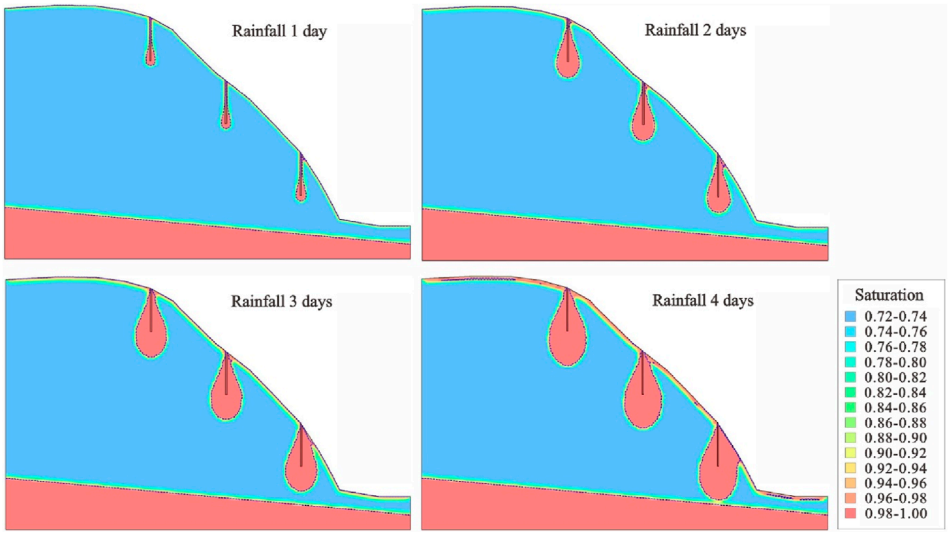

FIGURE 11
Saturation maps of the three-crack model with the crack depth of 15 m under extreme rainfall (70 mm/d).

to calculate the changes in slope stability under different rainfall conditions (Wu et al., 2018).

3.2.1 Calculation model

The study is based on the loess slope north of Haihu Bridge in Xining. Due to the irregular distribution of preferential infiltration channels (referred to as "cracks") such as fissures, sinkholes, and others in loess slopes, which are generally present at the back, middle, and front of the slope, the cracks were categorized according to their positions as back, middle, and front. Based on the investigation data of typical fissures in the study area, the depth of cracks in the model was set to 10m, 15 m and 20m, and the width of cracks was uniformly set to 0.5 m. This study includes both crack and no-crack models, with 13 models, as shown in Table 1. Some model examples are shown in Figure 3.

3.2.2 Boundary conditions

The bottom of the model was set as a non-permeable boundary. The left and right boundaries below the groundwater level were set as constant head boundaries, and the left and right boundaries above the groundwater level were set as zero flux boundaries. The surface was set as a unit flux boundary to simulate rainfall conditions. The potential seepage face method was employed, allowing excess rainfall to be converted into runoff. It was assumed that the cracks were filled with water, and the top of the cracks was set as a pressure head.

3.2.3 Rainfall conditions

This calculation aimed to study the general infiltration patterns under rainfall, so actual measured rainfall data was not used. Instead, two rainfall scenarios were modeled: normal rainfall and extreme

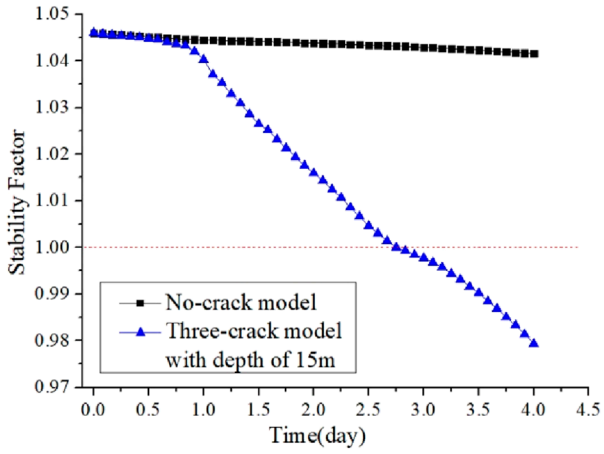

FIGURE 12
Stability factor curve of the three-crack model with the crack depth of 15 m under extreme rainfall (70 mm/d).

rainfall. Based on years of observational data, the rain intensity was set for normal rainfall at 30 mm/d, lasting 4 days. The intensity was set at 70 mm/d for extreme rain, with a 4-day duration. These two scenarios were used to analyze their impact on loess slope stability (Yang et al., 2016).

3.2.4 Calculation parameters

The soil-water characteristic curves of loess were obtained by indoor soil-water characteristic tests and the saturated permeability coefficients of loess were obtained by indoor infiltration tests. The infiltration parameters for the loess are shown in Figure 4. The geotechnical parameters used in the slope stability calculations are as follows: loess: unit weight = 13.6 kN/m^3, cohesion = 33.5 kPa, internal friction angle = 24.5 (Zhang S et al., 2017).

4 Results and discussion

4.1 Analysis of uniform rainfall infiltration patterns

4.1.1 Field monitoring results of rainfall infiltration

Figure 5 shows the relationship between daily rainfall and soil moisture from May 15 to 10 June 2023. Except for some scattered rain, the main rainfall events were on May 23 (12 mm), May 24 (6 mm), and May 26 (20 mm). The graph shows that the rainfall on May 23 and May 24 did not cause any changes in soil moisture. However, after 20 mm of rain on May 26, the soil moisture at a depth of 0.3 m began to increase, rising from 16% to 21%, and then remained stable with a slight decreasing trend. The soil moisture at the other four depths showed little change, indicating that the rainfall of 20 mm on May 26 and 38 mm over 4 days did not affect the soil below 0.6 m (Yang et al., 2016).

Figure 6 shows the relationship between daily rainfall and soil moisture from June 10 to August 10. During this period, there were intermittent rainfall events. A continuous rainfall process started on June 11, but with small amounts, having little effect on soil moisture. On June 15, with 16 mm of rainfall, and another 7 mm on June 16, the soil moisture at 0.3 m began to increase from 19.5% to 24%, then decreased. On June 21, after 17 mm of rainfall, the soil moisture at 0.3 m increased slightly before gradually declining. By August 10, intermittent rainfall occurred, but the amounts were small, with the maximum daily rainfall being 12 mm. After each rainfall, the soil moisture at 0.3 m slightly increased and decreased. No significant change was observed at deeper depths except for a slight increase at 0.6 m after June 26, which then stabilized (Zhang Y et al., 2017).

Figure 7 shows the relationship between daily rainfall and soil moisture from August 10 to October 10. A period of rainfall began on August 10. Despite 13.2 mm of rain on August 14 and a cumulative 24.8 mm over the previous 5 days, soil moisture was not significantly changed. On August 17, with 14.2 mm of rainfall, the soil moisture at 0.3 m increased and continued for 3 days. Following rainfall on August 22 and 23 (14 mm and 5mm, respectively), the soil moisture at 0.3 m increased again for 2 days before decreasing.

An extreme rainfall event occurred on August 29, with a daily rainfall of 78 mm. The soil moisture at 0.3 m increased rapidly and decreased after the rainfall ceased. The soil moisture at 0.6 m increased rapidly on August 30 and then decreased. The soil moisture at 0.9 m began to increase on September 1 and continued to increase for 3 days and then stabilized, the water content of the soil at 1.2 m began to increase slowly and continuously from September 13. At 1.5m, no significant change in moisture was observed. This indicates that intense rainfall can significantly affect the soil moisture at depths of 0.9 m and above, but it has little impact below 1.2 m.

4.1.2 Numerical simulation results of uniform rainfall infiltration

Figure 8 shows the saturation maps of the loess slope at Haihu Bridge North under regular rainfall (30 mm/d). The statistics indicate that rainwater infiltrates downward from the surface without considering rapid infiltration channels. The infiltration is relatively extensive near the surface, which increases the soil saturation, but the saturation at deeper layers does not change significantly. This indicates that the infiltration depth is limited to the shallow surface. As rainfall continues, the saturated zone near the surface grows, with the saturation decreasing as the depth increases. Under regular rain, infiltration is slow, with little impact on deeper soil (Yang et al., 2016).

Figure 9 shows the saturation maps of the loess slope at Haihu Bridge North under extreme rainfall (70 mm/d). The results indicate that similar to the regular rainfall patterns, rainwater infiltrates downward from the surface without considering rapid infiltration channels, and the infiltration depth increases with rainfall duration. Compared to the 30 mm/d rainfall, the infiltration depth under extreme rainfall is more significant for the same duration. Still, the affected area remains limited to the shallow surface, with little impact on the deeper soil.

Figure 10a shows the most dangerous sliding surface of the Haihu Bridge North landslide, and Figure 10b shows the variation curve of the stability factor for the no-crack model under rainfall conditions. It can be observed that the depth of the sliding surface is about 20m, and the infiltration depth of rainwater is far less than the depth of the sliding surface. As the rainfall time increases, the stability factor decreases gradually, with a faster reduction during heavy rainfall. However, in general, rainfall has little impact on the

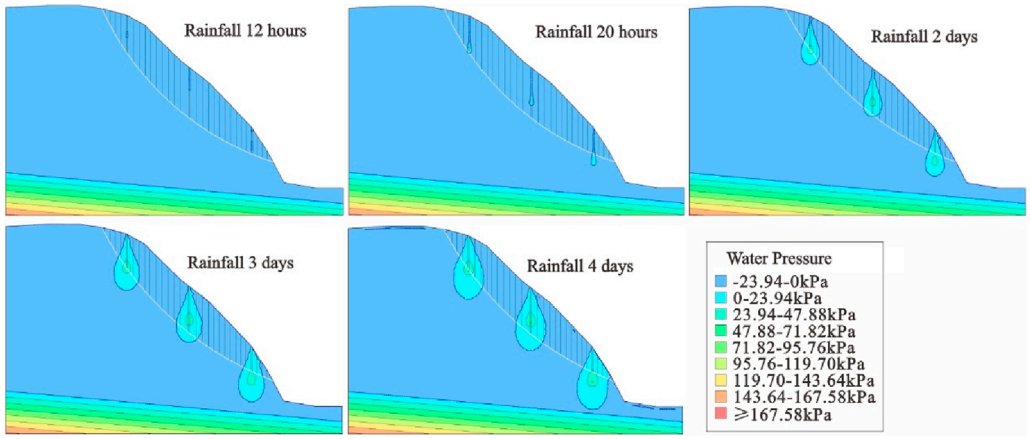

FIGURE 13
Water pressure cloud maps of the three-crack model with the crack depth of 15 m under extreme rainfall (70 mm/d).

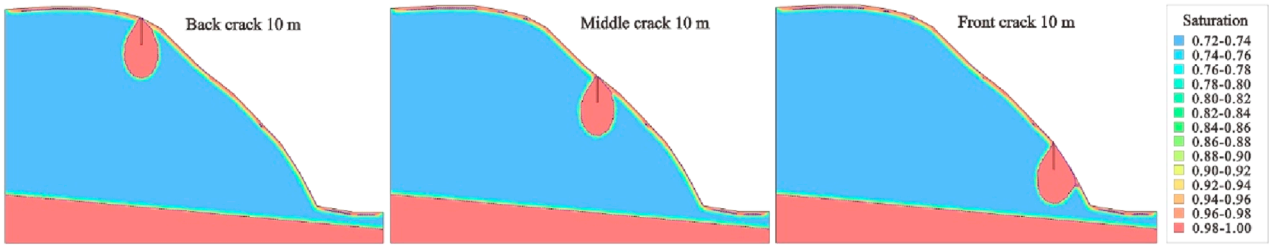

FIGURE 14
Saturation maps after 4 days of extreme rainfall for models with the crack depth of 10 m.

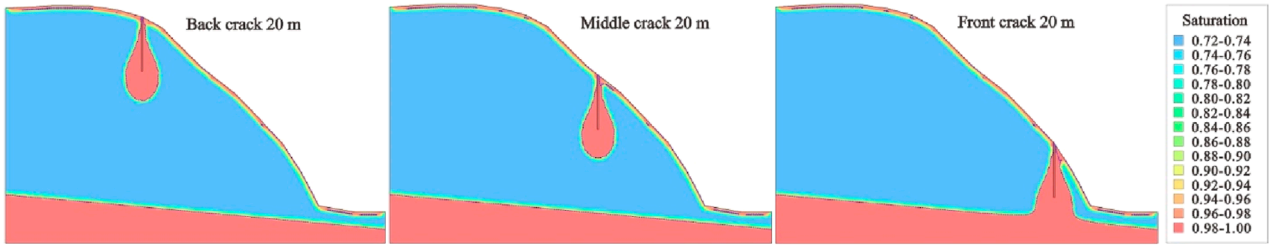

FIGURE 15
Saturation maps after 4 days of extreme rainfall for models with the crack depth of 20 m.

stability factor of the no-crack model, and the landslide does not become unstable (Li et al., 2018).

4.2 Analysis of rainfall infiltration patterns considering preferential infiltration channels

Taking the three-crack model, where cracks are distributed at the slope's back, middle, and front, as an example, the infiltration patterns with preferential infiltration channels are discussed. Figure 11 shows the saturation maps of the three-crack model with a crack depth of 15 m under extreme rainfall intensity (70 mm/d) for different rainfall duration. The results show that concentrated infiltration points form at all three cracks in the slope with cracks. Rainwater rapidly infiltrates, generating a transient saturated flow field near the cracks. This dramatically accelerates the infiltration rate. As rainfall continues, the saturated region expands from the vicinity of the cracks, forming a droplet-shaped saturated area.

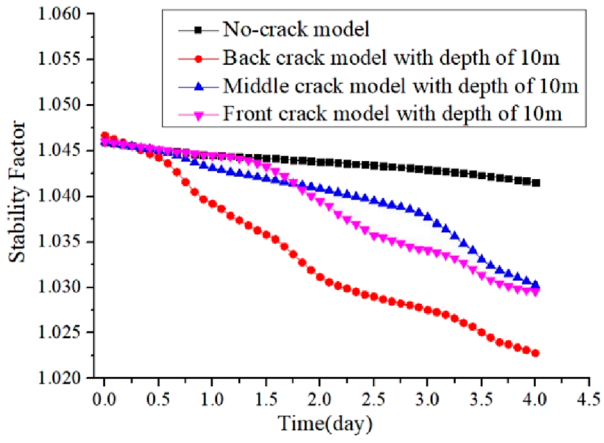

FIGURE 16
Stability factor variation curves of models (with a crack depth of 10 m).

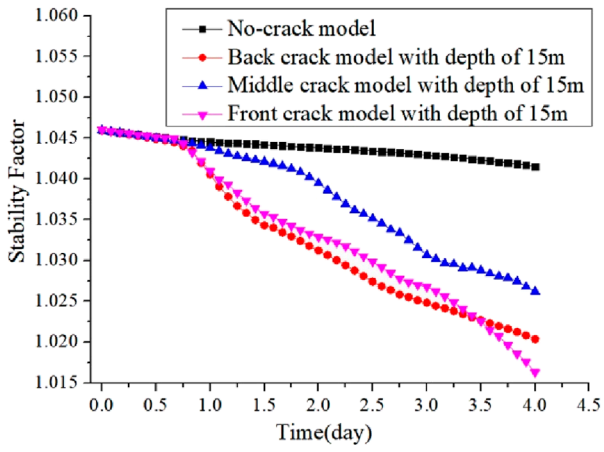

FIGURE 17
Stability factor variation curves of models (with a crack depth of 15 m).

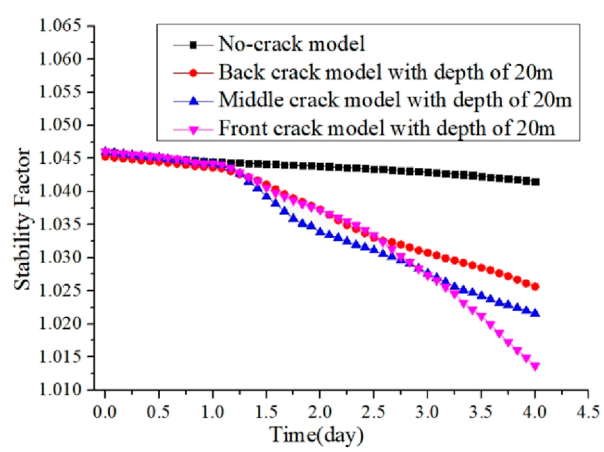

FIGURE 18
Stability factor variation curves of models (with a crack depth of 20 m).

Figure 12 shows the variation curve of the stability factor for the three-crack model with a crack depth of 15 m under extreme rainfall. Initially, the stability factor decreases slowly, but after 20 h of rainfall, the stability factor starts to decline rapidly. The stability factor reaches 1 after 2.75 days of rainfall, indicating that the landslide becomes unstable. In order to reveal the relationship between rainfall infiltration and landslide stability, the calculation results of rainfall time of 12 h, 20 h, 2 days, 3 days and 4 days were intercepted, as shown in Figure 13. After 12 h of rainfall, the saturated area is located near the crack (the blue dashed line in the figure is the demarcation line between the saturated and unsaturated area), because the depth of the crack in the model is 15m, which is smaller than the thickness of the slide, at this time, the saturated area has not yet arrived at the location of the slip surface, so the stability coefficient decreases to a small extent. After 20 h of rainfall, the saturated areas of the two cracks located at the back and front of the landslide reached the slip surface, and the stability coefficient began to decrease rapidly. Thereafter, with the continuation of the rainfall time, the saturated area continues to expand, and the length of the saturated section on the slip surface also continues to increase, and the stability coefficient continues to decrease until the landslide is unstable. The stable state of the landslide is mainly related to the mechanical properties of the slip surface, and the dominant infiltration channels in the slope can lead to rapid infiltration of rainfall into the slip surface, which reduces the shear strength of the slip surface, thus leading to the reduction of the stability of the landslide.

4.3 Influence of crack position and depth on landslide instability

A comparative analysis of crack models located at the back, middle, and front of the slope was conducted to clarify the impact of crack position on rainfall infiltration and slope stability. Figure 14 show the saturation maps after 4 days of extreme rainfall for various models at different positions with a depth of 10 m. The results indicate that the infiltration near the cracks forms a saturated region, and the size and shape of the saturated areas at different positions are similar, suggesting that the crack position has little effect on the rapid infiltration pattern.

Figure 15 show the saturation maps after 4 days of extreme rainfall for various models at different positions with a depth of 20 m. In the models with cracks located at the back and middle of the slope, the shape and size of the saturated area near the cracks are similar and droplet-shaped. In the model with cracks at the front of the slope, the shape of the saturated area is triangular. This is because the crack at the back and middle is farther from the groundwater level, and the rainwater infiltrates completely into the loess. In the front crack model, the crack is closer to the groundwater level, and the saturated region expands laterally when it reaches the groundwater level.

Figures 16–18 show the stability factor variations over time for various models. As observed in the 10 m deep crack model (Figure 16), the stability factor initially decreases slowly. After 14 h of rainfall, the stability factor of the back crack model starts to decline significantly. The front crack model experiences a rapid decrease after 1.5 days of rainfall, and the middle crack model

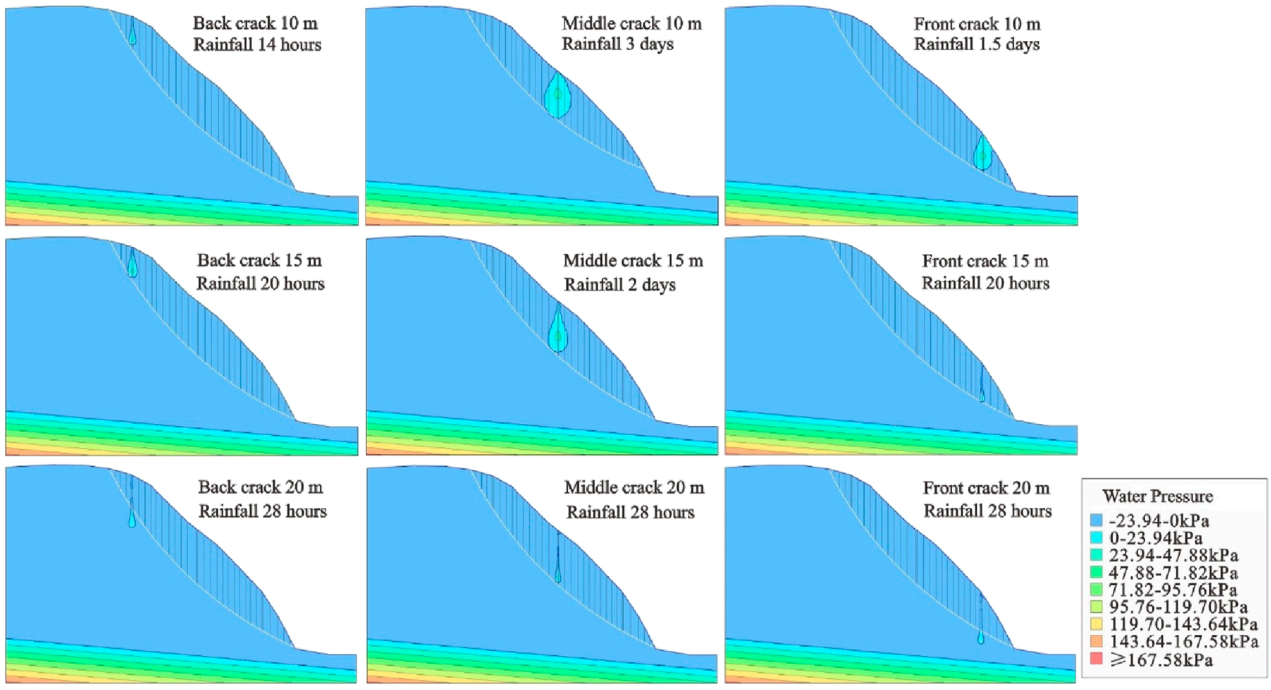

FIGURE 19
Water pressure cloud maps of the models.

TABLE 2 Statistical table for the distance from crack bottom to sliding surface and rainfall duration required for saturated region to reach sliding surface.

Models	Distance from crack bottom to sliding surface (m)	Rainfall duration required for saturated region to teaching sliding surface (h)
2	3.3	14
3	−1.7	20
4	−6.7	28
5	12.1	72
6	7.1	48
7	2.1	28
8	5.8	36
9	0.8	20
10	−4.2	28

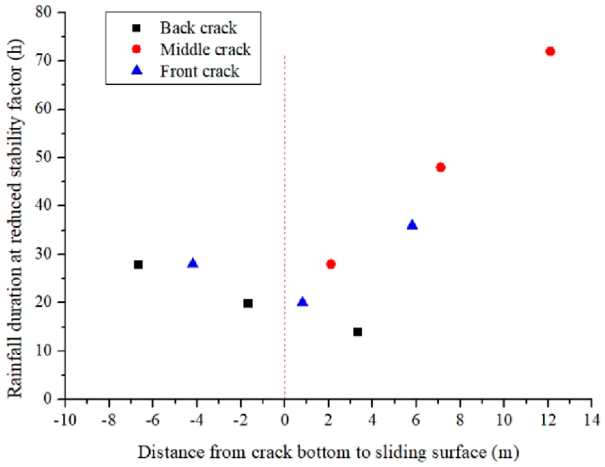

FIGURE 20
Plot of the distance from crack bottom to sliding surface with rainfall duration at reduced stability factor.

decreases considerably after 3 days. In the 15 m deep crack model shown in Figure 17, the back and front crack models have the same time for the significant decrease in stability factor, which is 20 h, and the middle crack model has a significant decrease in stability factor for 2 days. In the 20 m deep crack model shown in Figure 18, the time at which the model stability factor of the cracks at the three different locations start to decrease significantly is basically the same, 28 h after the rainfall. It can be seen that there is no uniform pattern between the location of the cracks and the change in the stability factor of the landslide. In order to further reveal the relationship between rainfall infiltration and landslide stability, the calculation results of the above rainfall time were extracted, as shown in Figure 19.

As can be seen from Figure 19, the time at which the stability factor of each of the above models started to decrease significantly was the moment when the saturated area near the cracks started to extend to the sliding surface, which further illustrates that the rapid infiltration of rainfall into the vicinity of the sliding surface is what led to the substantial decrease of the stability factor of the landslides. Since the sliding surface of the landslide in this study is in the shape of a circular arc, the bottom of the cracks at the same depth and at different locations are located at different distances from the sliding surface, resulting in inconsistencies in the length of rainfall required for rainfall infiltration to have a significant impact on the stability of the landslide. The statistical relationship between the distance of the bottom of the crack from the sliding surface and the rainfall time required for the saturated zone to reach the sliding surface is shown in Table 2 (positive values indicate that the bottom of the crack is above the sliding surface, negative values indicate that the bottom of the crack is below the sliding surface), and is plotted in Figure 20. Cracks closer to the sliding surface cause quicker reductions in the stability factor, with the time taken for the saturated region to reach the sliding surface being shorter. This pattern is more obvious when the cracks are located in the middle of the landslide. In this computational model, the sliding surface in the middle of the landslide is located deeper, and the bottoms of the cracks at the three depths of the setup are located above the slip surface, and the distance of the bottom of the cracks from the slip surface has a basically linear relationship with the length of the rainfall (the red points in Figure 20).

In conclusion, due to the limited infiltration capacity of loess, when preferential infiltration channels are not considered, the infiltration depth is shallow, and the impact on slope stability is small. However, common cracks and sinkholes in loess landslides enable rapid rainfall infiltration, which quickly reaches the slope body and forms a saturated region, reducing the shear strength and increasing the bulk density, especially when the saturated region reaches the sliding surface, resulting in a rapid decrease in the stability factor and leading to landslide instability. The position of preferential infiltration channels does not have a direct relationship with the stability factor reduction. Still, the distance between the crack bottom and the sliding surface significantly affects how rainfall affects slope stability. The closer the crack bottom is to the sliding surface, the more rapidly it affects slope stability.

5 Conclusion

On the basis of summarising the results of previous studies, this study focuses on the loess slopes in northern Xining, and carries out a series of systematic and in-depth studies on the stability of loess slopes under rainfall conditions. The model simplification is based on the generalisation of the survey data, and although there may be a slight deviation between the model and the actual situation, the results of this study are still of high practical value. Specifically, through field monitoring of rainfall and soil moisture, the study summarizes the changes in soil moisture under rainfall conditions. The SEEP/W module of the Geostudio software was used to simulate the infiltration patterns of unsaturated loess under different rainfall conditions. Finally, the SLOPE/W module was applied to analyze the stability of the slope under different rainfall conditions. The key conclusions are as follows.

5.1 Impact of uniform rainfall infiltration on soil moisture

The impact of uniform rainfall infiltration on soil moisture is limited in depth. Soil moisture at a depth of 0.3 m is significantly affected by rainfall. At 0.6m and 0.9 m depths, soil moisture is generally unaffected under smaller rainfall amounts. However, once the rainfall reaches a certain threshold, soil moisture in this depth range begins to change with continued infiltration, showing a delayed response relative to the 0.3 m depth. Soil moisture at depths greater than 1.2 m is generally unaffected by rainfall.

5.2 Effect of uniform rainfall infiltration on slope stability

Without considering rapid infiltration channels, rainwater infiltrates downward from the surface, and the infiltration depth increases gradually with the duration of rainfall. However, the infiltration impact is limited to the shallow surface layers, with minimal effect on the deeper soil and little impact on the slope's stability.

5.3 Impact of preferential infiltration channels on rainfall infiltration

Preferential infiltration channels significantly affect rainfall infiltration. Concentrated infiltration points form at the channels where rainwater rapidly infiltrates. A transient saturated flow field forms near the channels and spreads to surrounding areas. When the saturated region reaches the sliding surface, the slope's stability factor rapidly decreases, resulting in landslide instability.

These findings highlight the significant role that preferential infiltration channels play in the stability of loess slopes, particularly in the context of rainfall-induced instability. This study contributes valuable insights into understanding loess slope behavior under rainfall conditions and provides essential data for landslide prediction and risk management.

Data availability statement

The raw data supporting the conclusions of this article will be made available by the authors, without undue reservation.

Author contributions

GW: Conceptualization, Data curation, Investigation, Methodology, Project administration, Software, Writing – original draft. JY: Conceptualization, Funding acquisition, Investigation, Writing – review and editing. ZX: Data curation, Formal Analysis, Investigation, Software, Writing – review and editing. BL: Data curation, Software, Writing – review and editing. HQ: Investigation, Resources, Software, Validation, Writing – review and editing.

Funding

The author(s) declare that financial support was received for the research and/or publication of this article. This work was supported by Science and Technology Project of Qinghai 906 Engineering Survey and Design Institute (no. 2023-KJ-06), the Top Talents Program for High-End Innovative Talents in Qinghai Province (No. 2021-12), and the Scientific Research Projects of the Chinese Academy of Geological Sciences (HX2023-21).

Conflict of interest

The authors declare that the research was conducted in the absence of any commercial or financial relationships that could be construed as a potential conflict of interest.

Generative AI statement

The author(s) declare that no Generative AI was used in the creation of this manuscript.

Publisher's note

All claims expressed in this article are solely those of the authors and do not necessarily represent those of their affiliated organizations, or those of the publisher, the editors and the reviewers. Any product that may be evaluated in this article, or claim that may be made by its manufacturer, is not guaranteed or endorsed by the publisher.

References

Butler, D. L., and Gillham, R. W. (1996). The role of preferential flow in the development of landslides. *Can. Geotechnical J.* 33 (5), 761–772.

Chen, F., Wang, L., and Li, G. (2019). Numerical simulation of rainfall-induced infiltration in loess slopes and its impact on slope stability. *Landslides* 16 (4), 773–785.

Duan, Z., Song, K., Zhang, N., Zheng, L. C., Yan, X. S., and Zhang, M. M. (2024). Characteristics and mechanisms of soil structure damage under salt weathering. *Soil Tillage Res.* 238, 106030. doi:10.1016/j.still.2024.106030

Feng, L. (2020). Rainfall-induced landslides and their influencing factors. *Geol. Hazards Environ. Prot.* 31 (2), 85–92.

He, Q., Guo, F. Y., Li, R. D., Wang, L., Wang, W., Zhang, N., et al. (2023). Characteristics, mobility and dynamic of the Yahuokou flow-like landslide in Zhouqu, Gansu, China. *Gansu, China. Landslides* 20, 629–643. doi:10.1007/s10346-022-02000-8

He, Q., Wang, Y., Wang, W. P., Xu, W., Zhao, G., Chen, L., et al. (2024). Mechanism of the November 2018 landslide at the Kunming landfill and the geotechnical engineering risk control in the process of urbanization. *Bull. Eng. Geol. Environ.* 83, 196. doi:10.1007/s10064-024-03703-z

Hou, D., Zeng, F., Deng, J., Wei, H., and Xu, R. (2024). Failure mechanism of loess landslide induced by water stagnation on the combined surface. *Front. Earth Sci.* 12. doi:10.3389/feart.2024.1467209

Hu, Y. Z. (2013). *Soil mechanics and foundation engineering*. Beijing: Higher Education Press.

Kang, D. H., Lee, H., and Kim, M. (2017). Numerical simulation of rainfall infiltration and its effect on slope stability in loess deposits. *Environ. Geol.* 56 (5), 939–950.

Li, T., Wang, J. H., and Yang, J. H. (2020). Impact of rainfall characteristics on loess slope failure in northwestern China. *J. Civ. Eng.* 53 (3), 123–132.

Li, T., Wang, X. M., and Zhao, B. (2018a). Numerical simulation of rainfall-induced instability of loess slopes. *J. Eng. Geol.* 26 (6), 689–701.

Li, T., Zhang, Y., and Liu, J. (2018b). The effect of rainfall on loess slope stability and its application in risk assessment. *Geol. J.* 55 (1), 134–146.

Liu, F., Deng, Y., Zhang, T., Qian, F., Yang, N., Teng, H., et al. (2024). Landslide distribution and development characteristics in the beiluo river basin. *Land* 13, 1038. doi:10.3390/land13071038

Mirus, B. B., and Benda, L. (2010). Influence of rainfall patterns on landslide dynamics in the Pacific Northwest. *J. Hydrology* 397 (1-2), 1–14.

Wang, Y., He, Q., Wang, W., Zhang, N., Chen, L., Liu, Z., et al. (2024). Analysis on the mechanism and dynamics of frequent debris flows in typical alpine gorges areas—a case study of Yizhong river in Deqin County, Yunnan, China. *Front. Earth Sci.* 12, 1418763. doi:10.3389/feart.2024.1418763

Wu, H., Zhang, Z., and Yang, X. (2018). Mechanisms of preferential infiltration and slope stability under rainfall conditions: a numerical study. *Environ. Earth Sci.* 77 (6), 178.

Wu, J., Wang, L., and Zhou, H. (2015). The study of geological hazards in loess areas and the impact of anthropogenic activities. *J. Environ. Geol.* 68 (4), 897–906.

Yan, J. K., Huang, J. B., Li, H. L., Chen, L., and Zhang, Y. L. (2020). Study on instability mechanism of shallow landslide caused by typhoon and heavy rain. *J. Geomechanics* 26 (4), 481–491.

Yang, H., Liu, L., and Zhang, S. (2016). Study on soil-water characteristics and infiltration in loess areas. *J. Hydrology* 536, 73–81.

Zhang, S. S., Li, T., and Wang, L. (2019). Impact of preferential flow on landslide stability in loess regions. *Environ. Geol.* 28 (4), 240–249.

Zhang S, S., Yang, X., and Liu, Y. (2017). Analysis of rainfall-induced landslides and soil moisture dynamics in loess regions. *Landslides* 14 (6), 809–818.

Zhang Y, Y., Li, T., and Chen, J. (2017). Effect of rainfall intensity and duration on loess slope stability in Northwest China. *Geotechnical Test. J.* 40 (2), 317–328.

Zheng, S. H., Li, T., and Zhang, S. S. (2007). Development of fractures in loess areas and their effect on landslide instability. *J. Geomechanics* 13 (5), 45–53.